INDONESIAN JOURNAL ON GEOSCIENCE
Geological Agency
Ministry of Energy and Mineral Resources

Journal homepage: http://ijog.geologi.esdm.go.id
ISSN 2355-9314, e-ISSN 2355-9306

Seismicity Pattern of the Great Sumatran Fault System from Hypocenter Relocation of Regional Seismic Network

Ade Surya Putra[1], Andri Dian Nugraha[2], David P. Sahara[2], Zulfakriza[2], Nanang T. Puspito[2], Faiz Muttaqy[1], Pepen Supendi[3], and Daryono[3]

[1]Doctoral Program of Geophysical Engineering, Institut Teknologi Bandung, 40132, Indonesia
[2]Global Geophysics Research Group, FTTM, Institut Teknologi Bandung, 40132, Indonesia
[3]Agency for Meteorology, Climatology and Geophysics, Jalan Angkasa I, No.2, Kemayoran, Jakarta, Indonesia

Corresponding author: adexaputra@students.itb.ac.id
Manuscript received: December, 12, 2020; revised: February, 23, 2021;
approved: November, 19, 2022; available online: February, 10, 2023

Abstract - The seismicity pattern along the Great Sumatran Fault (GSF) was analyzed during April 2009 - December 2017 period with magnitude of ≥3.0 and depth of < 30 km. Of 752 preliminary absolute locations, 695 were successfully relocated using double-difference method to provide an improved view of seismicity, sharpening locations and interpretations of seismogenic features throughout the region. The relocation results depict a pattern of significant increase on small to intermediate earthquakes occurring in a shallow part of northern Sumatra, *i.e.* the Aceh and Seulimeum segments, as well as in central Sumatra, *i.e.* the Toru and Barumun. This increase was interpreted due to indications of creeping that reduce or prevent stress build-up on these segments. Meanwhile, few segments, *i.e.* the Tripa segment in the northern part, then Suliti and Siulak segments in the central part, and Manna segment in the southern part of Sumatra show the least activities over the period. These segments were identified as lock asperity, which caused accumulating stress that could be released as an earthquake. The behaviour of these locking segments can be related to the seismic gap along the GSF which has not experienced major earthquakes (M≥7) since 2000, making the densely populated area around these segments potentially have a great seismic hazard in the future.

Keywords: Great Sumatra Fault, hypocentre, relocation, double-difference method

© IJOG - 2023

How to cite this article:
Putra, A.S., Nugraha, A.D., Sahara, D.P., Zulfakriza, Puspito, N.T., Muttaqy, F., Supendi, P., and Daryono, 2023. Seismicity Pattern of the Great Sumatran Fault System from Hypocenter Relocation of Regional Seismic Network. *Indonesian Journal on Geoscience*, 10 (1), p.83-96. DOI: 10.17014/ijog.10.1.83-96

Introduction

Background

The Great Sumatran Fault (GSF) is well known as a highly segmented trench-parallel strike-slip fault as the result of oblique subduction between Indo-Australian Plate and Eurasian Plate (Sieh and Natawidjaja, 2000). The measurement of slip rates along the GSF based on the latest modeling using a combination of geological and geodetic methods carried out by Bradley *et al.* (2017) denotes that the slip rate in the Sumatran fault is around 14 mm/year.

The subduction zone between Indo-Australian Plate and Eurasian Plate forms an oblique convergent pattern. The tilt movement is the resultant of the two forces between downward movement and lateral movement. The downward movement is caused by the subduction of the Indo-Australian Ocean Plate under the Eurasian Plate. Whereas

lateral movements are reflected from the patterns of shear faults that form a series of structures of the right-lateral strike-slip fault on the mainland of Sumatra (McCaffrey, 2009). The impact of oblique convergent movement produced high seismicity along the GSF. Another study by Sieh and Natawidjaja (2000) proposed GSF segmented by geometrical irregularities into nineteen major segments, and few segments have large earthquakes occurred near the fault line (Figure 1).

Based on the historical earthquake data, the largest earthquake occurred in June 1943. This doublet earthquakes have occurred repeatedly on Sianok and Sumani segments. Estimated magnitudes on the second event magnitude M_s 7.6 following the first event of M_s 7.3 (Hurukawa *et al*., 2014). Historical earthquake data recorded the doublet earthquake shave also happened several times in GSF. First in 1926 with magnitude 6.8 in the Sumani segment and magnitude 6.5 in the Sianok segment. Then in 1943 with M 7.1 in the Sumani segment and M 7.3 in the Suliti segment. The last event was in 2007 with M 6.4 in the Sumani segment and M 6.3 in the Sianok segment (Untung *et al*., 1985; Natawidjaja and Triyoso, 2007; Nakano *et al*., 2010; Daryono *et al*., 2012; Hurukawa *et al*., 2014).

The motion of tectonic plates produces stresses on faults which cause earthquakes. It is known that the transferred stress between faults plays an important role in triggering earthquakes (Nakano *et al*., 2010; Zahradník and Sokos, 2013; Nissen *et al*., 2016; Bie *et al*., 2018; Momeni and Tatar, 2018). Nevertheless, there is still not much information about accurate locations due to earthquakes in this studied area (Nakano *et al*., 2010). The relocation along the Sumatran fault was previously done by Nugraha *et al*. (2018) using seismic catalog data by Indonesian Agency for Meteorology, Climatology, and Geophysics (BMKG). The results were focused on the subduction zone, so it did not discuss much about the pattern of seismicity behaviour in the Sumatran fault segment. The initial hypocentre by automatic picking on BMKG catalog had limitations in terms of spatial resolution, and accuracy of the hypocentre location which still showed the presence of artifacts, where some earthquakes were fixed at a depth of 10 km.

In this study, the initial hypocentre was determined using a nonlinear method and hypocentre relocation with a double-difference algorithm by utilizing P- and S-phase arrivals from occurrence of shallow earthquakes along nineteen segments of the GSF to enhance the spatial resolution of seismic activity, and get relatively more accurate location of earthquake hypocentre distribution. Using well-located seismicity distribution, the fault continuation can be delineated both laterally

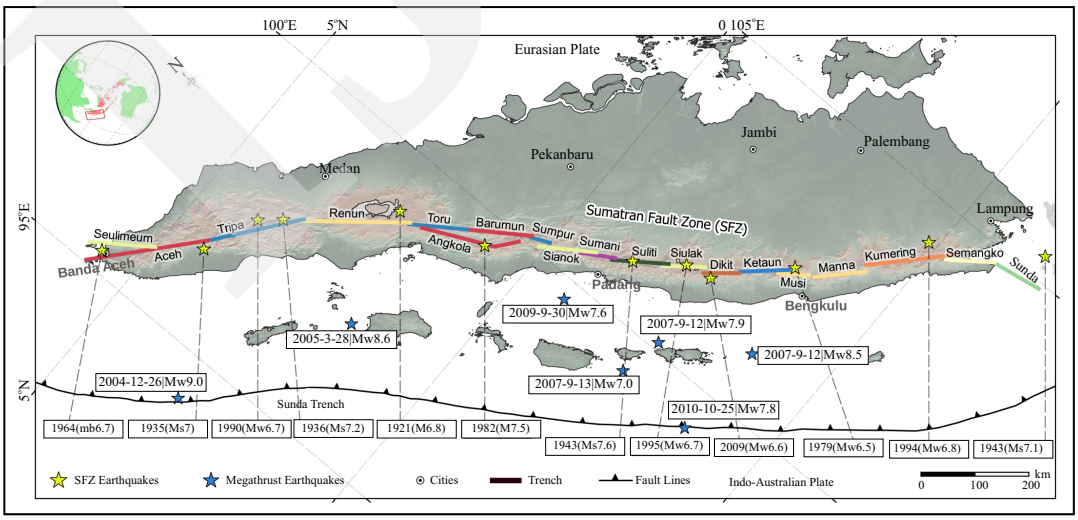

Figure 1. Historical earthquakes in Sumatra. Yellow star symbols indicate historical GSF earthquakes with M>6. Blue star symbols indicate historical megathrust earthquakes with M≥6.5 after 2004. Colour straight lines indicate the GSF segmented by geometrical irregularities into nineteen major segments by Sieh and Natawidjaja (2000).

and in depth, which also can image a fault line covered and hidden by thick sediments. The purpose of this study is to identify relations between seismicity through catalog of relatively accurate hypocentre relocations with historical major earthquake and indication of creeping or locked in GSF segments. This study aims to examine the seismicity pattern and fault interaction that may support seismic hazard mitigation along the GSF.

Material and Methods

The data used in this study is a data waveform originating from fifty-three seismometer networks scattered throughout Sumatra Island from Indonesian Agency for Meteorology, Climatology, and Geophysics (BMKG), with a recording period from April 2009 to December 2017. Data segmentation was then carried out to retrieve earthquake events near nineteen segments of GSF with criteria including depth of ≤ 30 km, magnitude of ≥ M3, and signal recording at a minimum of four stations, with clear wave phases and P- and S-phase arrivals were manually picked carefully using Seisgram2K (Lomax *et al*., 2009).

First, preliminary absolute earthquake locations were calculated using the probabilistic nonlinear earthquake location algorithm that implemented in NonLinLoc programme developed by Lomax *et al*., 2000; Lomax and Curtis, 2001; Lomax, 2005; Lomax *et al*., 2009; Lomax and Savvaidis, 2021) with seismic velocity model AK135 by Kennett *et al.* (1995). The double-difference relative relocation algorithm was applied in HypoDD programme generated by Waldhauser (2001) to refine the locations of the initial earthquakes. The double-difference technique leverages the fact that if the hypocentral separation between two earthquakes is relatively small in comparison to the event-station distance and the scale length of velocity heterogeneity. Then, the ray paths between the source region and a common station are similar along almost the entire ray path, and the difference in travel times for two events observed at one station can be attributed to the spatial offset between the events as shown on Figure 2. The HypoDD programme double-difference algorithm has been repeatedly tested using data from permanent networks and aftershock arrays across the world to validate its capacity to improve the representation of seismicity (Wu *et al*., 2008; Waldhauser and Schaff, 2008; Hauksson *et al*., 2012; Weller *et al*., 2012; Ramdhan *et al*., 2017; Rosalia *et al.*, 2019).

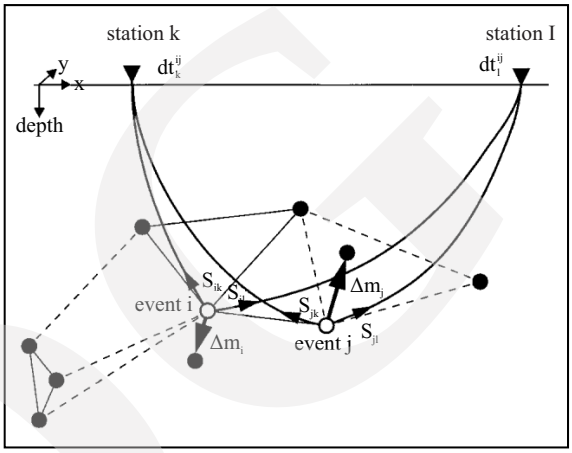

Figure 2. Schematic diagram of an illustration of the double-difference relocation algorithm. For two events, i and j, the initial locations (open circles), relocations (solid circles), and corresponding ray paths to a station k are shown. Thick arrows (Δmi and Δmj) indicate the corresponding relocation vectors (Adapted from Waldhauser and Ellsworth, 2000).

Results and Discussions

Phases 4198 P and phases 3979 S which have carefully been repicked (see an example manually picking of 21 January 2013 event in Figure 3(A), showed connection between event with near stations and far stations which recorded in Figure 3(B), and a Wadati Diagram was used to objectively evaluate the linear connection between phase data Figure 4(B) to provide quality control throughout the selection process; a Vp/Vs ratio of 1.7577 was achieved. 752 shallow events have successfully been located (depth less than 30 km) along nineteen segments of Sumatran fault with relatively accurate using nonlinier inversion method by oct-tree algorithm.

The initial velocity model 1D by AK135 with a modified layer depth was used to determine the initial locations (Kennett *et al*., 1995), drawing

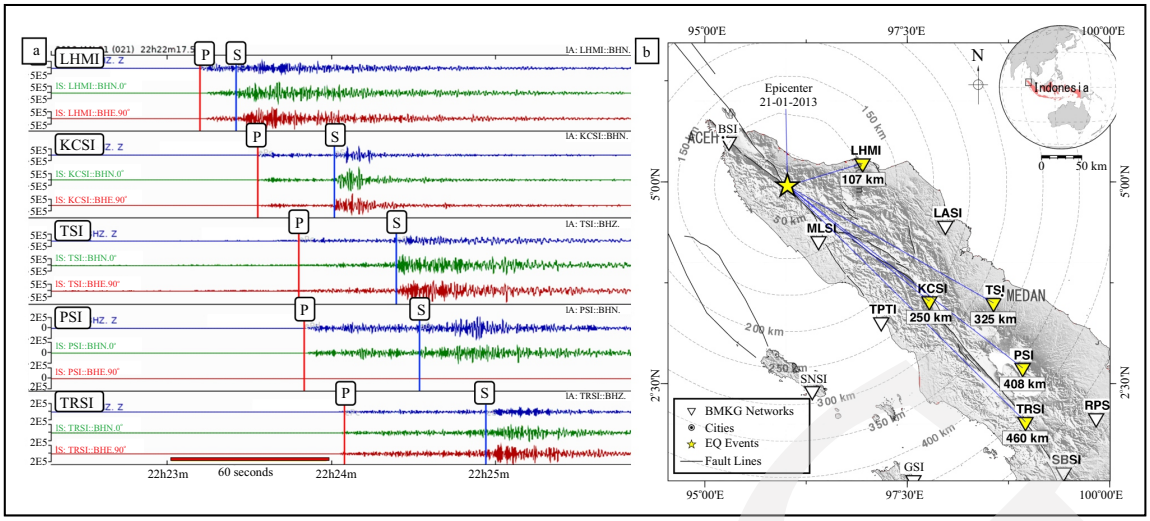

Figure 3. (a) Three-component seismogram examples of 21st January 2013 event, recorded at stations LHMI, KCSI, TSI, PSI, and TRSI. Red and blue lines indicate the picks of P- and S-wave arrival times, respectively. (b) Location of earthquake epicentres with recording stations of 21st January 13 events.

on earlier studies that had successfully applied to the Sumatra regional region, *i.e.* Engdahl *et al*. (2007) and Pesicek *et al*. (2010). The initial location determination results revealed that Root Mean Square (RMS) error was relatively better compared to RMS of BMKG catalog, which utilized 1D velocity model by IASP91 as shown in Figure 5. This result shows the importance of the velocity models in minimizing location errors.

As a result, the findings of this initial location determination were treated as a dataset of uncorrected absolute hypocentre positions, and the modified velocity model as inputs for HypoDD. The relocation process successfully refines 695 events from the 767 initial locations used. To ensure the relocation results have been carried out properly, the residual arrival time P- and S-wave was analyzed and compared with the residual results of arrival time before being relocated. The histograms of residual arrival times before relocation (Figure 6, left) and after relocation (Figure 6, right) for 695 events show that the relocation result has statistically improved with residual times, and are closer to zero compared to initial locations.

Following Waldhauser and Ellsworth (2000), estimating the relative location uncertainties of relocated events was evaluated by using bootstrap resampling method. This process is repeated a hundred times using 0.1 s standard deviation of pick arrival time. The result gives relative horizontal (longitude/x and latitude/y) bootstrap error ellipses at the 90% confidence level. Through relocation result, events can consistently be relocated by using eight stations in averages as shown in Figure 7 b3 with mean location errors of < 10 km as shown in Figure 7 b1 and b2. To analyze in more detail the relocation results, the relocated events were divided and compared with initial BMKG location into three regions including northern, central, and southern Sumatra. These regions represent the density of seismicity distributions along the GSF. The horizontal and vertical sections of seismicity map for these regions are shown in Figure 8. Based on the distribution of relocated seismicity, the northern Sumatra region is relatively more active than other regions in Sumatran fault. It is assumed that significant increase of seismicity in northern Sumatra, precisely near the boundary of Seulimeum segment and Aceh segment, is probably associated with stress changes in these areas. If this is connected to co- and post-seismic stress perturbations from megathrust earthquakes, Qiu and Chan (2019) found from previous megathrust earthquakes that stress in most segments of the Sumatran fault increased (stress changes are high/> 1 bar), except for the segment close to the Mentawai gap and few of southern Sumatra segments, where the stress level was only moderately elevated. The

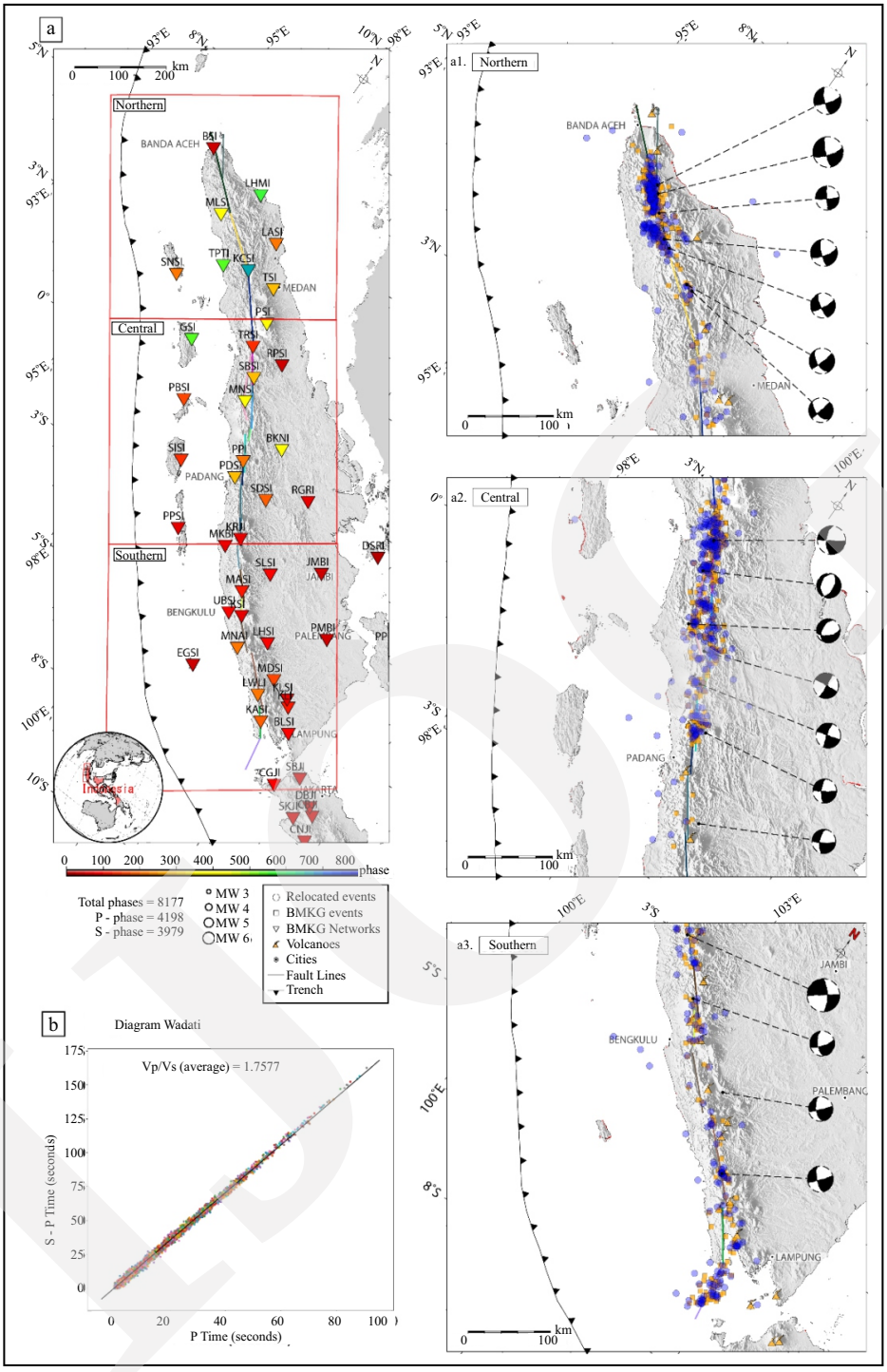

Figure 4. (a) Map illustrating the BMKG network distribution (inverted triangles) used in this study, as well as the GSF fault segment (line with different colours). Each station colour represents the number of phases selected (a1); (a2); (a3). From focal mechanism data collected by GCMT (Dziewonski *et al*., 1981; Ekström *et al.* (2012), almost along the GSF segment area can be seen dominated by earthquakes with a strike-slip mechanism pattern. The orange squares indicate earthquakes from the BMKG catalog, while the blue circles indicate earthquakes after relocation. (b) Wadati Diagram showing a linear relationship between picked phases. The Vp/Vs ratio in this study is 1.7577.

deep after slip following great earthquakes on subduction zone further enhanced the stress level at the Sumatran Fault in the Aceh segments.

Previous study by Hurukawa *et al*. (2014) identified six earthquakes of M ≥ 6.0 occurred in the northern Sumatra (as shown in Figure 1). Two

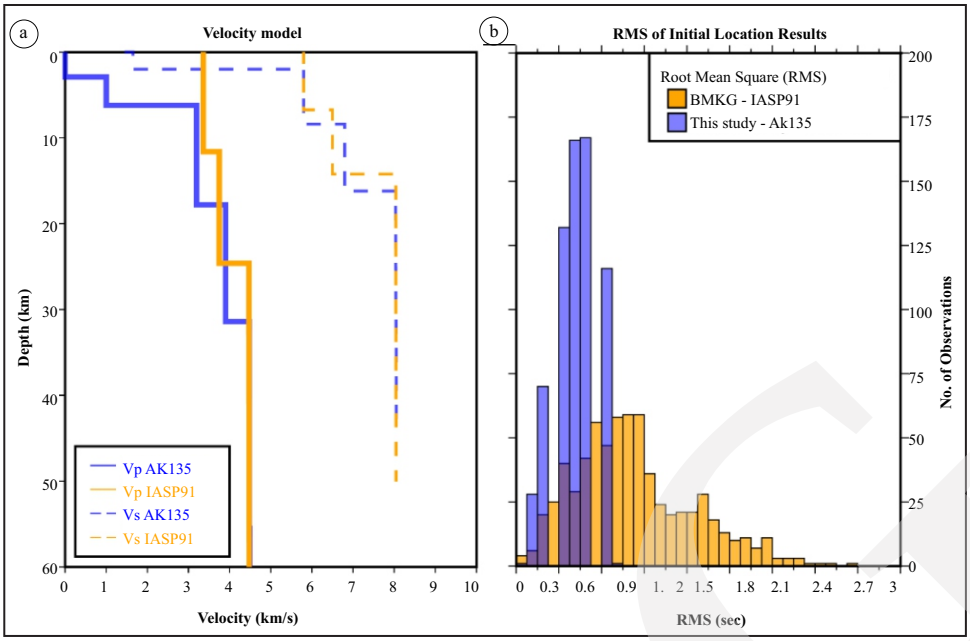

Figure 5. (a) 1D velocity model compared which utilized for initial location estimation (straight lines indicate Vp and dotted lines indicate Vs) (b) Histogram root mean square (RMS) error of travel time residuals obtained with IASP91 (Kennet, 1991) and AK135 (Kennett *et al*., 1995). 1D velocity model (orange colour indicate IASP91 model and blue colour indicate modified AK135 model used in this study).

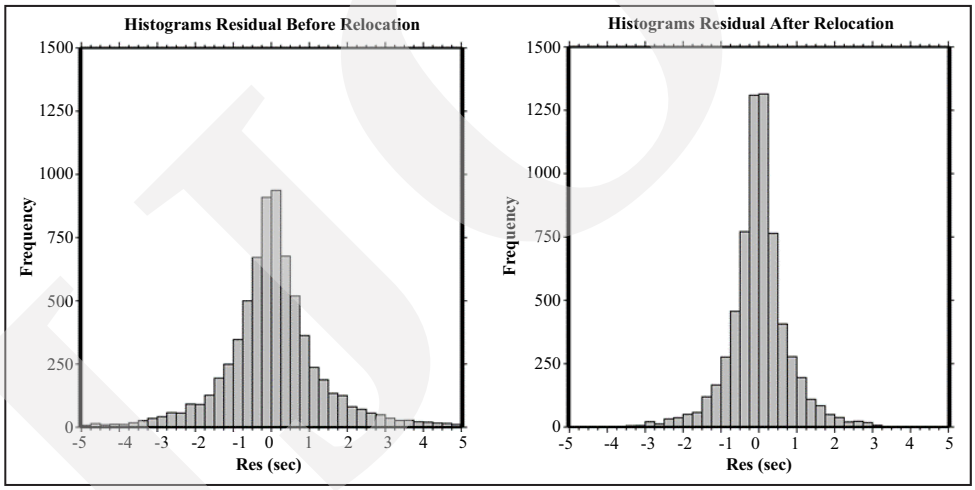

Figure 6. Histogram of arrival-time residuals before relocation (left part), and after relocation (right part) for 695 events.

earthquakes with M_s 7 in 1936 and m_b 6.7 in 1964, the 1935 M_s 7 occurred close to the Seulimeum segment and Aceh segment, damaged the area surrounding the Banda Aceh City located between those segments. Relocation results in vertical cross-section in northern Sumatra as illustrated in Figure 9 show better earthquake clustering and several lineations. GPS network observation by Ito *et al*. (2012) indicates shallow aseismic creep and deeper locking zone with creeping rate reaching 20 mm/year in this area (Ito *et al*., 2012; Tong *et al*., 2018). Earthquake activity was speculated occurred on the central part of near boundary of Seulimeum segment and Aceh segment (dotted rectangular/a as shown in Figure 8 b2).

In the central Sumatra region, the relocation results show a cluster of earthquake events in the branching area between the Toru, Angkola, and Barumun segments. A fairly good cluster was also formed in the Sianok and Sumani segments

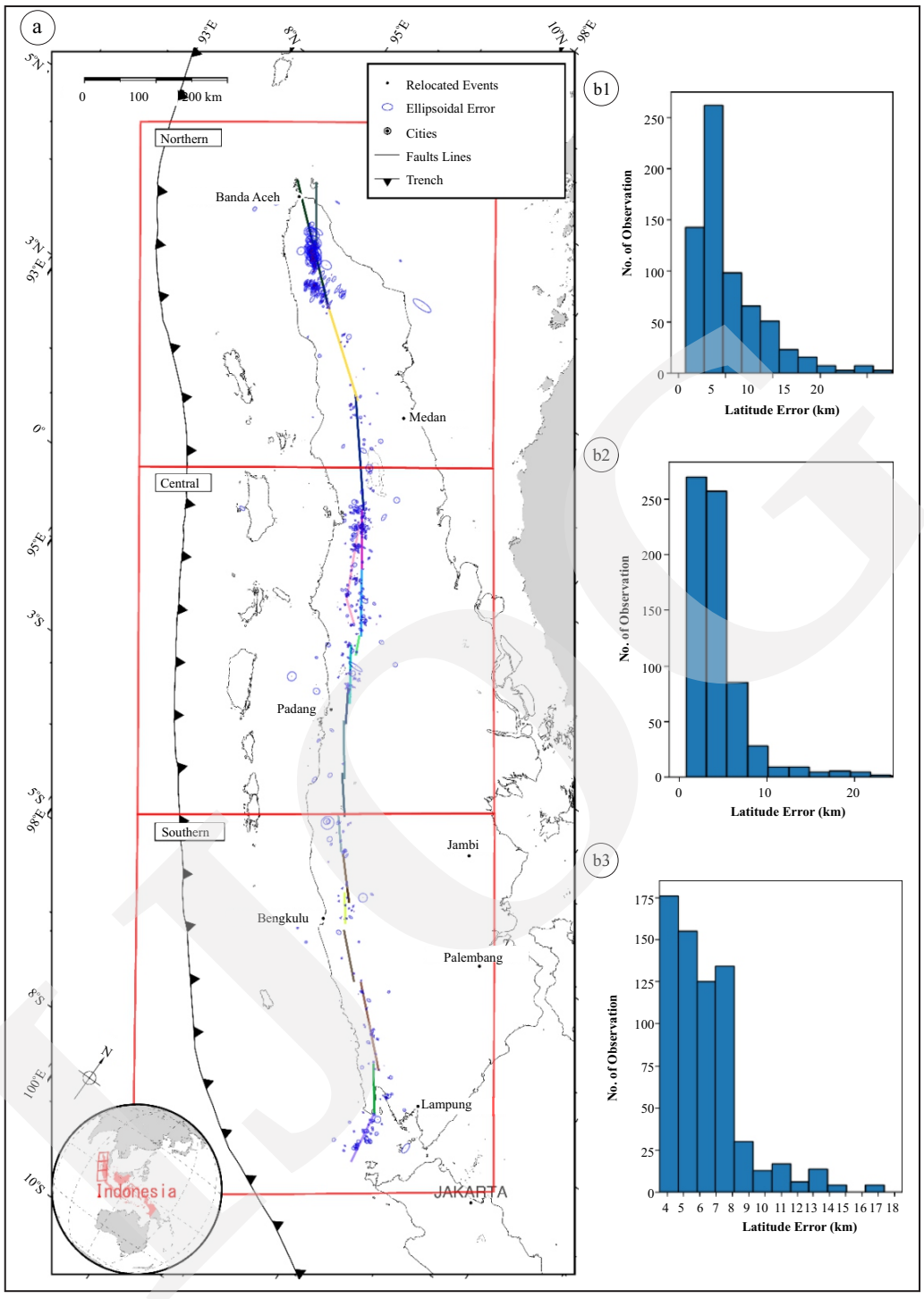

Figure 7. (a) Map showing relocation uncertainties of 681 events, ellipse symbol represents the errors from horizontal direction obtained by bootstrap analysis, rotated triangle represents seismic station. (b1) and (b2) represent the longitude and latitude errors (km) of relocated events. (b3) Number of stations used when relocating the event.

(dotted rectangular (c) as shown in Figure 8 b2). Cattin *et al*. (2009) also found the GFS most of the events prior to and after 2004 are located around Toru, Angkola, and Barumun branching area (1.8˚N). Their study also relates an increase of Coulomb stress and the particularly geometry of the Sumatran fault in this area. This branching area between Toru, Angkola, and Barumun segment in Sieh and Natawidjaja (2000) was observed as the greatest irregularity where the fault splits into two

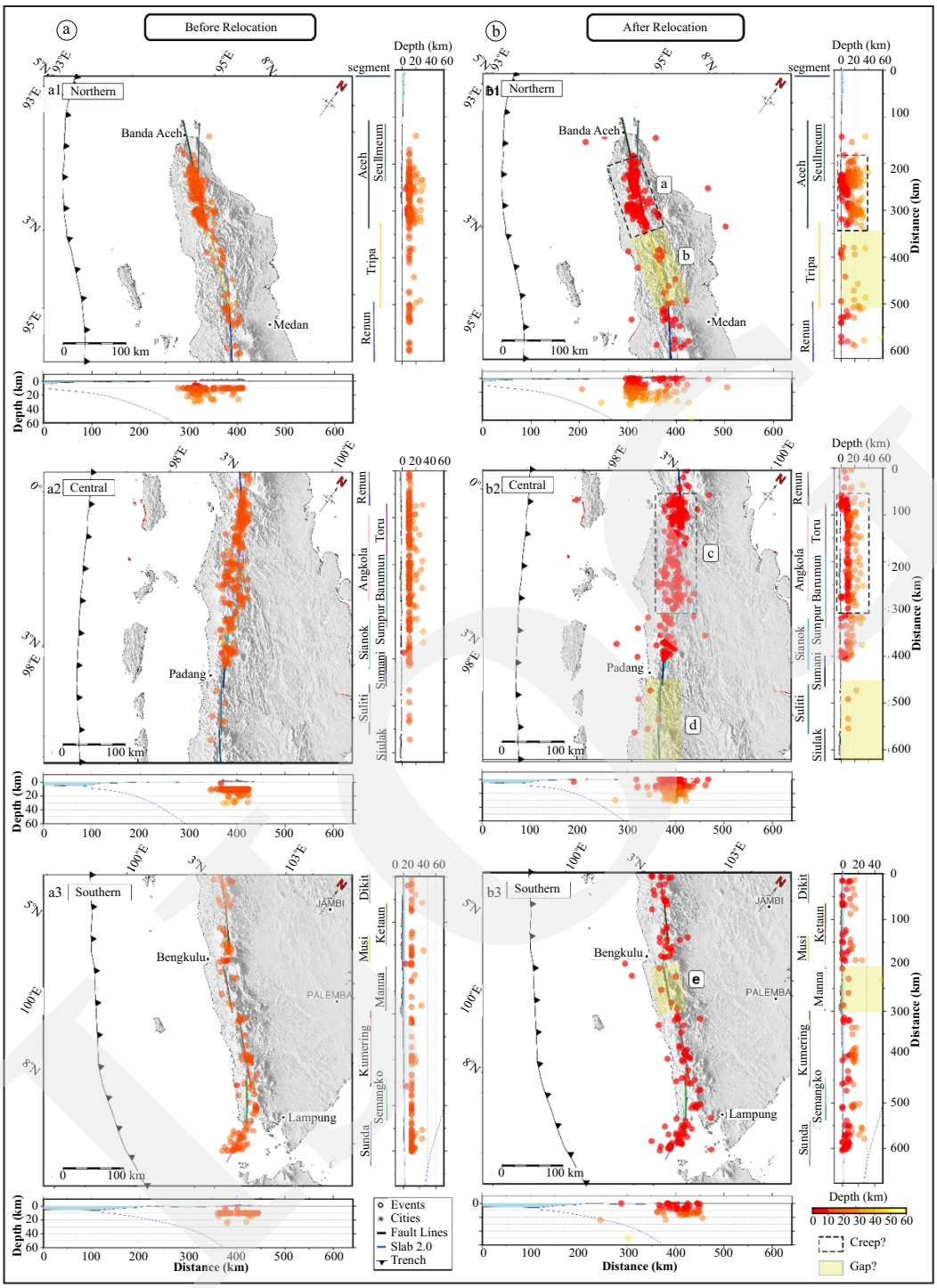

Figure 8. Distribution of seismicity in horizontal and vertical section (A) before relocation and (B) after relocation in northern, central, and southern Sumatra. Coloured vertical straight lines indicate GSF segments. Circle indicates earthquakes hypocentre after relocation. Light-green rectangulars indicate a presume of seismic gap on (b) Tripa segment, (d) Suliti and Siulak segments, and (e) Manna segment. Dotted rectangulars indicate a significant increase in seismicity interpreted as creeping on (a) Aceh-Seulimeum segments and (c) Toru-Angkola-Barumun segments. The blue line is Slab 2.0 which shows Sumatra subduction (Hayes *et al*., 2018).

subparallel strands up to 35 km apart or known as 'equatorial bifurcation'. This zone is suspected to provide the most stress heterogenity and seismic activity along GSF (Genrich *et al*., 2000; Sahara and Widiyantoro, 2019; Sieh and Natawidjaja, 2000). The ΔCFF >0 was resulted by Cattin *et al*.

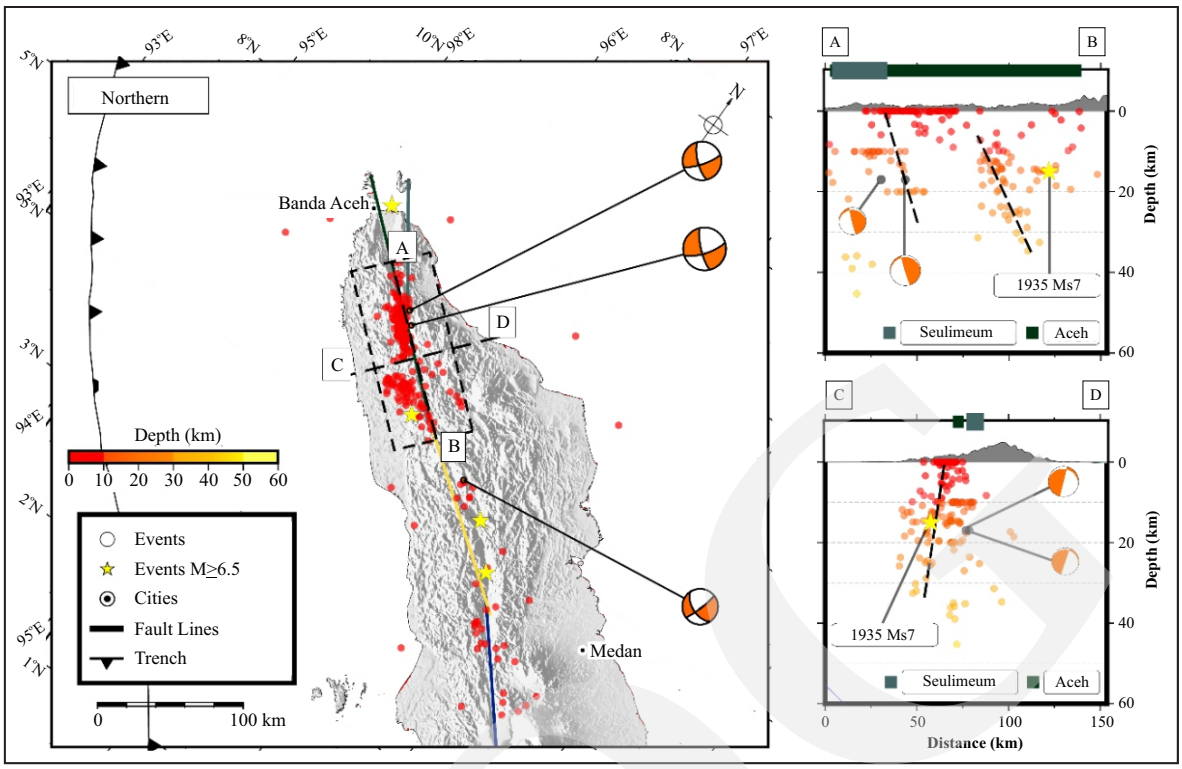

Figure 9. Map showing seismicity of northern Sumatra with focal mechanism data collected by GCMT (Dziewonski *et al.*, 1981; Ekström *et al.*, 2012), cross section A – B, C – D showing lineation (black dotted line) interpreted from correlation between cluster pattern, focal depth and history of major events. Coloured lines indicate GSF segments and star symbols indicate earthquakes of M ≥ 6.5.

(2009) along these two branches, except on the southernmost part of the Angkola segment. Therefore, this cluster activity is assumed experiencing an implication of structural irregularity, and release of stress as creeping earthquakes which occurred as a post-seismic relaxation following the 2004 megathrust earthquake.

The relocation result in vertical cross-section in central Sumatra region as shown in Figure 10 also shows cluster events that is close to the 1921 earthquake (M 6.8) located at the northwestern end of the Toru segment. The 1982 earthquake (M 7.5) and the cluster event on Sianok and Sumani segments is close to the 2007 doublet earthquakes (M 6.4 and M 6.3) (Hurukawa *et al.*, 2014; Nakano e*t al.*, 2010). Whereas in southern Sumatra, Qiu and Chan (2019) found near the 2007 Bengkulu rupture, the patch of seismicity rate before 2004 was low, especially in the northern part. There was almost no earthquake activity, while seismicity rate in the southern part was moderate. Similarly, after the Bengkulu rupture, seismicitiy after relocation results show quite good distribution on the Kumering segment and Semangko segment in Sumatran fault, although in some other segments in the southern Sumatra, especially on Manna segment, the seismic activity is as very low as on Tripa segment in the northern Sumatra and Suliti and Siulak segments on central Sumatra regions [light-green rectangulars (b), (d), and (e) in Figure 8 B]. The seismicity rate immediately jumps above the background rate, and continue to rise following the earthquake. The Sumatran fault was also elevated by post-seismic relaxation following the 2007 earthquake (Wiseman and Burgmann, 2011), but their seismicity status was found to show a seismic gap between other studied areas. Following latest major earthquake in this region, this region was interpreted to become locked and still accumulated the stress.

The relocation result along the GSF develop a pattern of fault behaviour in the form of creeping or locking based on seismic activity indicated by various segments in each region. The cause of this

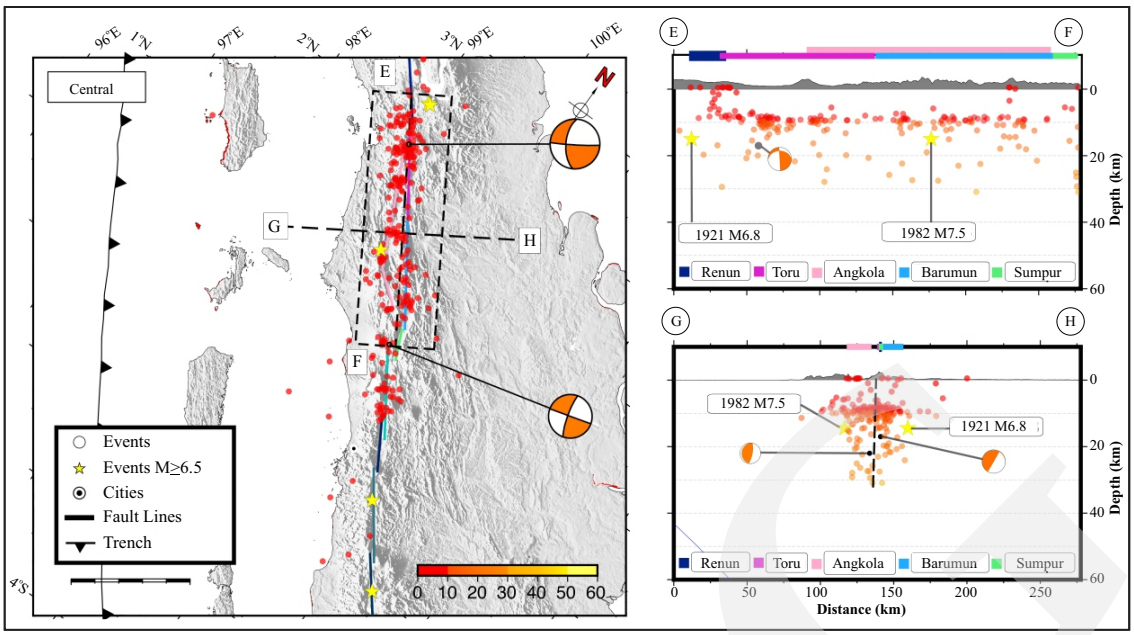

Figure 10. Map showing seismicity of central Sumatra with focal mechanism data collected by GCMT (Dziewonski *et al*., 1981; Ekström *et al*., 2012), cross section E – F, G – H showing lineation (black dotted line) interpreted from correlation among cluster pattern, focal depth, and history of major events. Coloured lines indicate GSF segments and star symbols indicate earthquakes of M ≥ 6.5.

increase in seismic activity may occur due to the influence of tectonic movements between plates, or it may also be a long series of seismic energy release processes from large earthquakes that previously occurred along the GSF or originating from megathrust earthquakes that previously occurred. This assumption is supported based on previous research by Qiu and Chan (2019) which found that an increase in seismicity and an increase in stress levels (> 1 bar) in most segments of the Sumatra fault, in the rupture area occurred after the megathrust earthquakes of 2004, 2005, 2007, and 2010. Seismicity continued to accumulate over a period of postseismic relaxation time.

Conclusions

Of 752, 695 shallow events have successfully been relocated (depth ≤ 30 km) along nineteen segments of along the GSF by using double-difference method. An overview of increased seismicity pattern was obtained as a creeping activity formed a fault lineation that correlated with relocation results, focal depth, and history of major earthquakes in GSF segments, especially on Aceh and Seulimeum segments in northern Sumatra and on Renun, Angkola, and Barumun segments in central Sumatra.

Instead, other segments, such as Tripa, Suliti, Siulak, and Manna segments, were actually experienced a significant decrease in activity. This segment was figured around probably locked and formed a seismic gap which could be accumulating the stress from previous major earthquakes and tectonic movement, and could have released into earthquakes of great magnitude in the future. However, further studies are needed to be able to estimate the probability of earthquake occurrence in all of GSF segments due to the stress feedback from the transient postseismic processes have not finished yet, and it will continue loading the Sumatran fault and the surrounding area in the years or decades to come.

Acknowledgment

We are thankful to Indonesian Agency for Meteorology, Climatology, and Geophysics (BMKG)

for the waveform and catalog data. We are also grateful to PMDSU 2017 scholarship from the Ministry of Research, Technology, and Higher Education of the Republic of Indonesia awarded to ASP. Most figures were produced using the Global Mapping Tools (Wessel and Smith, 1991), and QGIS (GIS Development Team, 2013).

References

Bie, L., Hicks, S., Garth, T., Gonzalez, P., and Rietbrock, A., 2018. 'Two go together': Near-simultaneous moment release of two asperities during the 2016 Mw 6.6 Muji, China earthquake. *Earth and Planetary Science Letters*, 491, p.34-42. DOI: 10.1016/j.epsl.2018.03.033.

Bradley, K.E., Feng, L., Hill, E.M., Natawidjaja, D.H., and Sieh, K., 2017. Implications of the diffuse deformation of the Indian Ocean lithosphere for slip partitioning of oblique plate convergence in Sumatra: Sumatran Slip Partitioning. *Journal of Geophysical Research: Solid Earth*, 122, p.572-591. DOI: 10.1002/2016JB013549.

Cattin, R., Chamot-Rooke, N., Pubellier, M., Rabaute, A., Delescluse, M., Vigny, C., Fleitout, L., and Dubernet, P., 2009. Stress change and effective friction coefficient along the Sumatra-Andaman-Sagaing fault system after the 26th December 2004 (M_w = 9.2) and the 28th March 2005 (M_w = 8.7) earthquakes: STRESS CHANGE ALONG SUMATRA-ANDAMAN-SAGAING FAULT SYSTEM. *Geochemistry, Geophysics, Geosystems*, 10, p.1-21. DOI: 10.1029/2008GC002167.

Daryono, M.R., Natawidjaja, D.H., and Sieh, K., 2012. Twin-Surface Ruptures of the March 2007 M>6 Earthquake Doublet on the Sumatran Fault. *Bulletin of the Seismological Society of America*, 102, p.2356-2367. DOI:10.1785/0120110220.

Dziewonski, A.M., Chou, T.A., and Woodhouse, J.H., 1981. Determination of earthquake source parameters from waveform data for studies of global and regional seismicity. *Journal of Geophysical Research: Solid Earth*, 86, p.2825-2852. DOI:10.1029/JB086iB04p02825.

Ekström, G., Nettles, M., and Dziewoński, A.M., 2012. The global CMT project 2004-2010: Centroid-moment tensors for 13,017 earthquakes. *Physics of the Earth and Planetary Interiors*, 200-201, p.1-9. DOI:10.1016/j.pepi.2012.04.002.

Engdahl, E. R., Villasenor, A., DeShon, H. R., and Thurber, C. H., 2007. Teleseismic Relocation and Assessment of Seismicity (1918-2005) in the Region of the 2004 Mw 9.0 Sumatra-Andaman and 2005 Mw 8.6 Nias Island Great Earthquakes. *Bulletin of the Seismological Society of America*, 97(1A), p.S43-S61. DOI: 10.1785/0120050614

Genrich, J.F., Bock, Y., McCaffrey, R., Prawirodirdjo, L., Stevens, C.W., Puntodewo, S.S.O., Subarya, C., and Wdowinski, S., 2000. Distribution of slip at the northern Sumatran fault system. *Journal of Geophysical Research: Solid Earth*, 105, p.28327-28341. DOI: 10.1029/2000JB900158.

GIS Development Team, Q., 2013. QGIS Geographic Information System. Open Source Geospatial Foundation.

Hardebeck, J. and Husen, S., 2010. Earthquake location accuracy. *Community Online Resource for Statistical Seismicity Analysis*. DOI: 10.5078/corssa-55815573.

Hauksson, E., Yang, W., and Shearer, P., 2012. Waveform Relocated Earthquake Catalog for Southern California (1981 to June 2011). *Bulletin of the Seismological Society of America*, 102 (5), p2239-2244. DOI: 10.1785/0120120010

Hayes, G.P., Moore, G.L., Portner, D.E., Hearne, M., Flamme, H., Furtney, M., and Smoczyk, G.M., 2018. Slab2, a comprehensive subduction zone geometry model. *Science*, 362, 58pp. DOI:10.1126/science.aat4723.

Hurukawa, N., Wulandari, B.R., and Kasahara, M., 2014. Earthquake History of the Sumatran Fault, Indonesia, since 1892, Derived from

Relocation of Large Earthquakes. *Bulletin of the Seismological Society of America*, 104, p.1750-1762. DOI:10.1785/0120130201.

International Seismological Centre, 2020. *ISC Bulletin*. DOI:10.31905/D808B830.

Ito, T., Gunawan, E., Kimata, F., Tabei, T., Simons, M., Meilano, I., Agustan, Ohta, Y., Nurdin, I., and Sugiyanto, D., 2012. Isolating along-strike variations in the depth extent of shallow creep and fault locking on the northern Great Sumatran Fault: ALONG-STRIKE VARIATIONS ON THE GSF. *Journal of Geophysical Research: Solid Earth*, 117, DOI:10.1029/2011JB008940.

Kennet, B. L. N., 1991. IASPEI 1991 SEISMOLOGICAL TABLES. *Terra Nova*, 3 (2), p.122-122. DOI: 10.1111/j.1365-3121.1991.tb00863.x

Kennett, B.L.N., Engdahl, E.R., and Buland, R., 1995. Constraints on seismic velocities in the Earth from traveltimes. *Geophysical Journal International*, 122, p.108-124. DOI:10.1111/j.1365-246X.1995.tb03540.x.

Lomax, A., and Curtis, A., 2001. Fast probabilistic earthquake location in 3D models using Oct-Tree importance sampling. *Geophysical Research Abstracts*, 3.

Lomax, A., 2005. A Reanalysis of the Hypocentral Location and Related Observations for the Great 1906 California Earthquake. *Bulletin of the Seismological Society of America*, 95 (3), p.861-877. DOI: 10.1785/0120040141

Lomax, A., Michelini, A., and Curtis, A., 2009. Earthquake location, direct, global-search methods. *Encyclopedia of Complexity and Systems Science: Assembles for the First Time the Concepts and Tools for Analyzing Complex Systems in a Wide Range of Fields*, p.2449-2473.

Lomax, A., Virieux, J., Volant, P., and Berge-Thierry, C., 2000. Probabilistic Earthquake Location in 3D and Layered Models, *In*: Thurber, C.H., Rabinowitz, N. (eds.), Advances in Seismic Event Location. Springer, Dordrecht, p.101-134. DOI:10.1007/978-94-015-9536-0_5.

Lomax, A., and Savvaidis, A., 2021. High-Precision Earthquake Location Using Source-Specific Station Terms and Inter-Event Waveform Similarity. *Journal of Geophysical Research: Solid Earth*, 127 (1). DOI: 10.1029/2021JB023190

McCaffrey, R., 2009. The Tectonic Framework of the Sumatran Subduction Zone. *Annual Review of Earth and Planetary Sciences*, 37, p.345-366. DOI:10.1146/annurev.earth.031208.100212.

Momeni, S.M. and Tatar, M., 2018. Mainshocks/aftershocks study of the August 2012 earthquake doublet on Ahar-Varzaghan complex fault system (NW Iran). *Physics of the Earth and Planetary Interiors*, 283, p.67-81. DOI:10.1016/j.pepi.2018.08.00.1.

Nakano, M., Kumagai, H., Toda, S., Ando, R., Yamashina, T., Inoue, H., and Sunarjo, 2010. Source model of an earthquake doublet that occurred in a pull-apart basin along the Sumatran fault, Indonesia. *Geophysical Journal International*, 181, p.141-153. DOI: 10.1111/j.1365-246X.2010.04511.x.

Natawidjaja, D.H., 2018. Updating active fault maps and sliprates along the Sumatran Fault Zone, Indonesia. *IOP Conference Series: Earth and Environmental Science*, 118, 012001pp. DOI:10.1088/1755-1315/118/1/012001.

Natawidjaja, D.H. and Triyoso, W., 2007. The Sumatran Fault Zone - From Source to Hazard. *Journal of Earthquake and Tsunami*, 01, p.21-47. DOI: 10.1142/S1793431107000031.

Nissen, E., Elliott, J., Sloan, R., Craig, T., Funning, G., Hutko, A.E., Parsons, B., and Wright, T.J., 2016. Limitations of rupture forecasting exposed by instantaneously triggered earthquake doublet. *Nature Geoscience,* 9 (4), p.330-336. DOI: 10.1038/ngeo2653.

Nugraha, A.D., Shiddiqi, H.A., Widiyantoro, S., Thurber, C.H., Pesicek, J.D., Zhang, H., Wiyono, S.H., Ramdhan, M., Wandono, and Irsyam, M., 2018. Hypocentre Relocation along the Sunda Arc in Indonesia, Using a 3D Seismic-Velocity Model. *Seismologi-*

cal Research Letters, 89, p.603-612. DOI: 10.1785/0220170107.

Pesicek, J. D., Thurber, C. H., Zhang, H., DeShon, H. R., Engdahl, E. R., and Widiyantoro, S., 2010. Teleseismic double-difference relocation of earthquakes along the Sumatra-Andaman subduction zone using a 3-D model. *Journal of Geophysical Research: Solid Earth*, 115 (B10). DOI: 10.1029/2010JB007443

Putra, A.S., Dian Nugraha, A., Puspito, N.T., and Triyoso, W., 2019. Preliminary Result of Hypocentre Relocation Using Double Difference Method along Sumatran Fault, Indonesia. *IOP Conference Series: Earth and Environmental Science*, 318 (1), 012009pp. DOI:10.1088/1755-1315/318/1/012009.

Qiu, Q. and Chan, C.H., 2019. Coulomb stress perturbation after great earthquakes in the Sumatran subduction zone: Potential impacts in the surrounding region. *Journal of Asian Earth Sciences*, 180, 103869. DOI:10.1016/j.jseaes.2019.103869.

Ramdhan, M., Widiyantoro, S., Nugraha, A. D., Métaxian, J.-P., Saepuloh, A., Kristyawan, S., Sembiring, A. S., Santoso, A. B., Laurin, A., and Fahmi, A. A., 2017. Relocation of hypocenters from DOMERAPI and BMKG networks: a preliminary result from DOMERAPI project. *Earthquake Science*, 30(2), p.67–79. DOI: 10.1007/s11589-017-0178-3

Rosalia, S., Widiyantoro, S., Dian Nugraha, A., Ash Shiddiqi, H., Supendi, P., and Wandono, 2017. Hypocentre Determination Using a Non-Linear Method for Events in West Java, Indonesia: A Preliminary Result. *IOP Conference Series: Earth and Environmental Science*, 62, 012052pp. DOI: 10.1088/1755-1315/62/1/012052.

Rosalia, S., Widiyantoro, S., Dian Nugraha, A., and Supendi, P., 2019. Double-difference tomography of P- and S-wave velocity structure beneath the western part of Java, Indonesia. *Earthquake Science*, 32, p.12-25. DOI: 10.29382/eqs-2019-0012-2.

Sahara, D. P., and Widiyantoro, S., 2019. The pattern of local stress heterogeneities along the central part of the Great Sumatran fault: A preliminary result. *Journal of Physics: Conference Series*, 1204, p.012091. DOI: 10.1088/1742-6596/1204/1/012091

Sieh, K. and Natawidjaja, D.H., 2000. Neotectonics of the Sumatran fault, Indonesia. *Journal of Geophysical Research: Solid Earth*, *105*, 28295-28326. DOI: 10.1029/2000JB900120.

Simanjuntak, A.V.H., Muksin, U., and Sipayung, R.M., 2018. Earthquake relocation using HypoDD Method to investigate active fault system in Southeast Aceh. *Journal of Physics: Conference Series*, 1116, 032033pp. DOI: 10.1088/1742-6596/1116/3/032033.

Tong, X., Sandwell, D.T., and Schmidt, D.A., 2018. Surface Creep Rate and Moment Accumulation Rate Along the Aceh Segment of the Sumatran Fault From L-band ALOS-1/PALSAR-1 Observations. *Geophysical Research Letters*, 45, p.3404-3412. DOI: 10.1002/2017GL076723.

Untung, M., Buyung, N., and Kertapati, E., 1985. Rupture along The Great Sumatran Fault, Indonesia, During The Earthquakes of 1926 and 1943. *Bulletin of the Seismological Society of America*, 75, p.313-317.

Waldhauser, F. and Ellsworth, W.L., 2000. A Double-Difference Earthquake Location Algorithm: Method and Application to the Northern Hayward Fault, California. *Bulletin of the Seismological Society of America*, 90, p.1353-1368. DOI: 10.1785/0120000006.

Waldhauser, F., 2001. *hypoDD -- A Program to Compute Double-Difference Hypocenter Locations* (USGS Numbered Series 2001–113). HypoDD-A Program to Compute Double-Difference Hypocenter Locations, 2001–113. DOI: 10.3133/ofr01113

Waldhauser, F., and Schaff, D. P., 2008. Large-scale relocation of two decades of Northern California seismicity using cross-correlation and double-difference methods: NORTHERN CALIFORNIA SEISMICITY RELOCATION. *Journal of Geophysical Research: Solid Earth*, 113(B8). DOI: 10.1029/2007JB005479

Weller, O., Lange, D., Tilmann, F., Natawidjaja, D., Rietbrock, A., Collings, R., and Gregory, L., 2012. The structure of the Sumatran Fault revealed by local seismicity: The structure of The Sumatran Fault. *Geophysical Research Letters*, 39 (1), p.1-7. DOI: 10.1029/2011GL050440.

Wessel, P. and Smith, W.H.F., 1991. Free software helps map and display data. *Eos, Transactions American Geophysical Union*, 72, p.441-446. DOI: 10.1029/90EO00319.

Weston, J., Engdahl, E.R., Harris, J., Di Giacomo, D., and Storchak, D.A., 2018. ISC-EHB: reconstruction of a robust earthquake data set. *Geophysical Journal International*, 214, p.474-484. DOI: 10.1093/gji/ggy155.

Wiseman, K. and Burgmann, R., 2011. Stress and Seismicity Changes on the Sunda Megathrust Preceding the 2007 Mw 8.4 Earthquake. *Bulletin of the Seismological Society of America*, 101, p.313-326. DOI:10.1785/0120100063.

Wu, Y.-M., Chang, C.-H., Zhao, L., Teng, T.-L., and Nakamura, M., 2008. A Comprehensive Relocation of Earthquakes in Taiwan from 1991 to 2005. *Bulletin of the Seismological Society of America*, 98(3), p.1471–1481. DOI: 10.1785/0120070166

Zahradník, J. and Sokos, E., 2013. The Mw 7.1 Van, Eastern Turkey, earthquake 2011: two-point source modelling by iterative deconvolution and non-negative least squares. *Geophysical Journal International*, 196, p.522-538. DOI:10.1093/gji/ggt386.